

Storage of CO₂ in depleted hydrocarbon reservoirs in low-permeability chalk

A GESTCO contribution

Niels Bech and Peter Frykman



Storage of CO₂ in depleted hydrocarbon reservoirs in low-permeability chalk

A GESTCO contribution

Niels Bech and Peter Frykman

Abstract

Depleted oil and gas reservoirs are candidates for underground CO₂ disposal. The Roar field is a high-porosity, low-permeability chalk carbonate reservoir in the Danish North Sea, and a detailed reservoir model has been used for a simulation study of the influencing factors during CO₂ injection.

Roar is an anticlinal structure, induced through tectonic uplift. The reservoir is located at a depth of 2000 m and covers an area of 14 km². The reservoir rock is chalk with porosities in the range of 35 – 45%. The matrix permeability is between 0.01 and 10 mD. There is only a few natural fractures. The accumulation consists of free gas and a thin oil zone. The gas contains condensate.

The ECLIPSE 100 reservoir simulator is used to predict the state of the reservoir after 16 years of production and to model the subsequent injection of CO₂ over a period of 30 years. Various CO₂ injection scenarios have been simulated and a number of factors and parameters are identified which have a considerable influence on the field injectivity and simulated results.

Introduction

This work is a contribution to GESTCO, an EU funded project for the exploration of the viability of wide-scale application of CO₂ storage to reduce CO₂ emissions in Europe. The principal objective of the GESTCO project is to make a major contribution to reducing the European emissions of CO₂ to the atmosphere. The project will aim at determining the true potential of subsurface storage for CO₂ in Europe through case studies from different regions.

Some of the promising geological structures for underground CO₂ disposal are depleted or near depleted oil and gas reservoirs, examples of which may be found in the Danish sector of the North Sea. Most Danish hydrocarbon reservoirs are composed of chalk carbonate which is characterised by very low matrix permeabilities, so low that one may fear that the injectivity is prohibitively low. Two fields, Roar and Tyra appear to be the most likely candidates as they exhibit relatively high matrix permeabilities of up to 10 mD. They are both gas condensate fields and contain only few natural fractures. The major difference is in size, Tyra being approximately ten times larger than Roar. We have selected Roar as subject of one of the Danish case studies and expect that the principal results apply to Tyra as well.

In the Ekofisk chalk reservoir in the Norwegian North sea excess gas was injected for almost 20 years, and was found to distribute through the natural fracture system and contact the reservoir fluids (Jakobson and Christian 1994). Little breakthrough was experienced and supported that the gas migrated into the chalk matrix. During the initial injection, eight wells on the crest of the field was converted to injectors, and the gas was injected at a field wide rate of 350-400x10⁶ scf/day.

In the present study various CO₂ injection scenarios have been simulated and a number of factors and parameters have been identified which have a considerable influence on the field injectivity and simulated results.

Due to limitations of the applied reservoir simulator (ECLIPSE 100) some of the results obtained particularly regarding storage capacity are considered preliminary only.

Furthermore, we have neglected possible reactions between the chalk matrix rock and CO₂ and enhanced recovery of hydrocarbons through CO₂ injection is not considered.

Roar Field

Roar is an anticlinal structure, induced through tectonic uplift. The reservoir is located in the North Sea at a depth of 2000 m and covers an area of 14 km². The reservoir rock is chalk with porosities in the range of 35 – 45%. The matrix permeability is between 0.01 and 10 mD. There is only a few natural fractures. The accumulation consists of free gas and a thin oil zone. The gas contains condensate. The field went on stream in 1996 and the estimated ultimate production volumes are 494x10⁹ scf (14x10⁹ sm³) of gas and 19x10⁶ stb (3x10⁶ sm³) of oil and condensate (Energistyrelsen 2002). The reservoir pressure is 4328 psi (29.8 Mpa).

Reservoir Simulation

The present study has utilised a standard industry black-oil reservoir simulator (ECLIPSE 100 (Schlumberger GeoQuest 2000)). It contains a miscible flood model based on the Todd-Longstaff mixing parameter model (Todd and Longstaff 1972). In relation to the modelling of CO₂ injection into a hydrocarbon reservoir it has a number of limitations:

- It can handle only two non-water components and one hydrocarbon phase. As one of these components is necessarily CO₂ there is room for one hydrocarbon component only which must be either dead oil or dry gas. But Roar contains both live oil and condensate gas. As a consequence, the approach adopted is such that:
 - The condensate gas is described as one of the non-water components while the injected CO₂ is the other.
 - The oil (including condensate) remaining in the reservoir at the end of the production period is modelled as condensate gas when the CO₂ injection starts.
- The simulator cannot describe the solubility of CO₂ in water, which may be a severe limitation.

Roar Simulation Model

Grid. The simulation model is based upon a geostatistical model of the Roar field with approximately 2,000,000 cells (Vejbæk 1999a and 1999b). The model has been upscaled with CMoSTM (If 2002) to grids containing 31x46x10 and 31x46x25 grid cells, respectively (Frykman 2002), see Fig. 1. The 31x46x10 cell model has been used in the present study. A bottom aquifer is included as an 11th layer. The total number of grid cells is thus

31x46x11 = 15686. The aquifer properties are: Thickness = 1000 ft, porosity = 20% and permeability = 0.6 mD.

Compressibility. Considerable complexity is related to compressibility as has been shown for high-porosity chalk reservoirs (Ruddy et al. 1989). One main point is the non-reversible nature of much of the chalk reservoir compressibility. Another is the impact of CO₂ injection on chalk mechanical compaction. Laboratory testing conducted to date indicates that introducing CO₂-charged injection water into Ekofisk chalk samples results in an immediate and vigorous dissolution reaction with large axial strains and high strain rates (Jensen, Harpole and Østhus 2000). No attempts have been made so far to assess the impact of CO₂ on pore volume compressibility.

In the present work the applied pore volume compressibility is equal to 5×10^{-5} 1/psi (7.25×10^{-9} 1/Pa). This value represents an average over the reservoir rock types as well as the range of pressure that the reservoir undergoes (Ruddy et al. 1989).

Saturation Functions. Relative permeabilities which are typical of chalk have been used. The irreducible water saturations are 0.11 and 0.05 in the Danian (upper four layers) and Maastrichtian, respectively. Irreducible gas saturations are zero and it is assumed that the relative permeabilities of the condensate gas-CO₂ mixture are equal to those of the condensate gas. The saturation scaled curves are shown in Fig. 2. Gas-water capillary pressures are assumed equal to zero.

PVT Data. The hydrocarbon and water PVT data are obtained from fluid samples from one the Roar-2 appraisal well. CO₂ data are computed by PVTsim (Calsep 2001). The formation volume factor and viscosity relationships are shown in Figs. 3 and 4.

History Match. The simulation model is history matched so that the calculated total hydrocarbon and water production ultimo 2000 approximately matches the recorded total volumes (Energistyrelsen 2002). The figures are given in Table 1 which also shows values computed by a pore volume compressibility of 5×10^{-6} 1/psi (7.25×10^{-10} 1/Pa). The reason for this is explained below.

Production and CO₂ Injection Scenarios

Production. The reservoir is depleted by three wells set in production January 1996 (R-3C), February 1996 (R-7B) and December 1999 (R-1), respectively. The selected production period is 16 years (i. e. until January 2012). Produced surface volumes during the 16 year production period are given in Table 2 together with the total produced reservoir volume and the reservoir pressure. The reservoir pressure has decreased from 4328 to 3566 psi (29.8 to 24.6 MPa).

CO₂ Injection. Three CO₂ injection cases have been considered:

- Injection in well R-3C
- Injection in a new drilled vertical well completed over the entire reservoir interval.

- Injection in all three horizontal wells under group control so that the rate to each well is proportional to its injection potential.

In all three cases the target injection rate is 63.5×10^6 scf/day (100 kg/sec or 3×10^6 tons/year) of CO₂ which according to Weir, White and Kissling 1996 is the typical amount of waste CO₂ from a 1000 MW thermal power plant. The maximum permitted bottom hole pressure was put equal to the initial reservoir pressure which was 4328 psi. The total injection period considered is 30 years.

Results and Discussion

Obtainable injection rates and injected total volumes are shown in Figs. 5 and 6. It is not surprising that the best result is obtained when injection takes place in the three horizontal wells. In this case the requested CO₂ injection rate of 63.5×10^6 scf/day (100 kg/sec) can be maintained for five years. The total amount of CO₂ injected during the 30 years period is 436×10^9 scf (12×10^9 sm³) corresponding to 22 million tons. The injected reservoir volume of CO₂ is 202×10^6 bbl (32×10^6 m³) which is 44% of the volume produced.

In the case with the single vertical injector the performance is not nearly as good. The requested CO₂ injection rate of 63.5×10^6 scf/day can not be achieved at all. Due to the small absolute permeability of the reservoir the effective Kh product and hence the injectivity of a vertical well is mediocre. The total amount of CO₂ which can be injected through the vertical well during the 30 years period is 69×10^9 scf (2×10^9 sm³) corresponding to 4 million tons.

The results obtained are of course subject to error due to simulator limitations as well as uncertainties in the specified input data. The neglect of the solubility of CO₂ in water probably has a conservative effect on the calculated results whereas it is more difficult to estimate the consequences of the simplified treatment of the fluids and components present. Yet it seems likely that the CO₂ storage capacity is overestimated when the free oil present in the reservoir at the start of the injection is neglected. This will be investigated in a second phase of this project (Bech and Frykman 2002) using the compositional simulator ECLIPSE 300 (Schlumberger GeoQuest 2000). Assuming that the basic geostatistical model is correct, some input data uncertainties are associated with

- Upscaled grid
- Rock or pore volume compressibility
- Saturation functions
- PVT data
- Initial state (at start of CO₂ injection)
- Max. permissible bottom hole pressure during injection
- Well outflow (skin)
- Aquifer strength and extension

Grid. The implication of refining the grid will be examined in the second phase of this work.

Compressibility. The rock compressibility used (5×10^{-5} 1/psi or 7.25×10^{-9} 1/Pa) is obtained from Ruddy et al. 1989 as an average value over the pore pressure range covered during the production period. However, it is a parameter which is subject to a large uncertainty. Besides pressure and rock type it depends strongly on porosity (Ruddy et al. 1989). The value used corresponds to a porosity around 39%. In other North Sea chalk field studies a value of 0.3×10^{-5} 1/psi (0.44×10^{-9} 1/Pa) has been used which according to Ruddy et al. 1989 corresponds to porosities around 30%. As the porosity variation within the reservoir is quite large it would be a definite improvement to apply porosity dependent pore volume compressibilities.

In order to evaluate the sensitivity of the calculated results to variations in the formation compressibility the case with CO₂ injection in the three horizontal wells was calculated using a pore volume compressibility of 0.5×10^{-5} 1/psi (0.73×10^{-9} 1/Pa). That is, the compressibility is reduced by a factor of 10. The calculated total production volumes and reservoir pressures are compared in Fig. 7. It is seen that the production of the highly compressible gas is only little affected whereas the oil production and in particular the water production is smaller. The smaller rock compressibility leads to a considerably larger pressure decline even though the totally produced volume is smaller. Results from the subsequent injection calculation are presented in Fig. 8. It is seen that the target injection rate can be maintained for a much longer period of time (17 years as opposed to 5) when the pore volume compressibility is small. The total amount of CO₂ injected during the 30 years is 35% larger.

Another factor which adds to the uncertainty is the question whether or not the elastic limit is exceeded. If yes, the assumption of reversibility does not hold. The pore compressibility curves depicted in Ruddy et al. 1989 indicate that the elastic stress limit is indeed exceeded at the pressure 3566 psi (24.6 Mpa) prevailing at the end of the production period. According to Ruddy et al. 1989: *"..if the stress is relaxed, the response curve does not retrace the original load path but rather follows an elastic path typical of a more consolidated (lower porosity) sample."* This means that it would probably be more correct to use a smaller pore compressibility during the CO₂ injection phase. In Fig. 9 is shown the results obtained when the production period is calculated with $C_{rock} = 5 \times 10^{-5}$ 1/psi and the CO₂ injection period is computed with $C_{rock} = 0.5 \times 10^{-5}$ 1/psi and $C_{rock} = 5 \times 10^{-5}$ 1/psi, respectively. The latter is definitely the worst of the three compressibility scenarios considered. The target injection rate can be maintained for just two years and the total amount of CO₂ injected is only 55% of the base case amount. It is evident that more work on rock compressibility behaviour of high-porosity chalk is required to improve the mathematical modelling.

Saturation Functions. The relative permeabilities affect the pressure gradients in the reservoir and hence the time of max. injection rate. Water and gas functions are based upon a general petrophysical chalk model developed by the operator and probably sufficiently accurate. The assumption that the relative permeability of the CO₂-condensate gas mixture equals that of the pure condensate gas seems more dubious. In order to evaluate the sensitivity of the calculated solution to variations in the gas mixture relative permeability the function is replaced by a straight line through (0,0) and (1,1) as shown in Fig. 10. The influence of variations in the gas relative permeability on the calculated solution is shown in Fig. 11. It is seen that the straight-line relative permeability leads to more favourable in

jection conditions. This is not surprising as the relative permeability in this case is higher over most of the saturation interval.

The residual saturations (end points) affect the storage capacity. It is expected however, that this effect is dominated by the uncertainty in the state of the reservoir after the 16 years of production.

Capillary pressure was assumed equal to zero. In production calculations this is standard procedure in case of gas/oil and gas/water systems because the capillary transition zone is small due to the large density difference. The situation may however be quite different in the injection case where e.g. mobile gas and water phases may coexist over much larger heights. The results in Fig. 12 are obtained by putting the gas-water capillary pressure equal to three times the oil-water capillary pressure (This corresponds approximately to the ratio between the interfacial tensions). It is seen that the influence of the gas-water capillary pressure is modest.

PVT Data. Gas and condensate PVT data are based upon analyses of fluid samples from the reservoir while the properties of the black oil have been calculated from standard correlations (Calsep 2001). There is no reason to believe that the uncertainties associated with the PVT properties have a substantial influence on the computed results.

The CO₂ data applied are valid for pure CO₂. Neither the composition of CO₂ gas from a power station nor the influence of impurities on the PVT properties are known at present.

Initial State. Prior to the initiation of the CO₂ injection the reservoir is produced for 16 years (1996 through 2011) by three horizontal production wells. The production phase is simulated by a model which has been history matched so that the calculated total hydrocarbon and water production ultimo 2000 approximately equals the recorded total volumes. It is obvious that there is large uncertainty associated with the predicted reservoir state at the time where production ends and injection starts. No attempts have been made to quantify the magnitude of this uncertainty.

Bottom Hole Pressure Limit. The imposed upper limit of the bottom hole pressure during injection has a direct influence on the time span during which the requested injection rate can be maintained. The higher the limit the longer the time span. In the present calculations the maximum permitted bottom hole pressure has been put equal to the initial reservoir pressure in order to provide a reasonable assurance against fracturing. It may be possible to apply a higher injection pressure if it can be demonstrated that the stresses leading to fracturing of the formation and/or the overburden are not exceeded (Foged 2001).

Well Outflow. In the present calculations it has been assumed that there is no skin. A negative skin will have a similar effect as an increased bottom hole pressure limit and hence increase the time period during which the requested injection rate can be maintained. A positive skin will have the opposite effect.

In Fig. 13 is shown results obtained with the skin factor equal to 0, 5 and 10, respectively. It is seen that a positive skin has a very negative influence on the injection conditions.

Aquifer Strength and Extension. Sensitivity to aquifer properties has been evaluated by increasing the aquifer permeability from 0.6 to 6mD and quadrupling its lateral extension, respectively. Both changes tend to improve the storage capabilities as shown in Fig. 14. However, the time span over which the requested CO₂ injection rate can be maintained is a little smaller in the high-permeability case than in the base case. This is probably a relative permeability effect.

Estimated CO₂ Storage Capacity. The Roar reservoir is far from completed after 16 years of production. If we assume an abandonment pressure of 3000 psi (21 MPa) the total reservoir volume of produced hydrocarbons is predicted to be 6.3×10^8 bbl or 1.0×10^8 m³. If it is further assumed that the produced hydrocarbon volume may be replaced by injected CO₂ then the estimated storage capacity of the Roar field is 76 million tons, the density of CO₂ at the initial reservoir pressure of 4328 psi (29.4 MPa) being 46 lb/ft³ (742 kg/m³).

Summary and Conclusions

The ultimate objective of the present work is to estimate to which extent tight chalk fields are useable for underground disposal of CO₂. Till this end the relatively small Roar condensate gas field was selected as a case study. So far, a number of factors and parameters have been identified which have a considerable influence on the field injectivity and simulated results.

The key factors/parameters are:

- **Total well Kh product**
Due to the small absolute permeability of the reservoir the well injectivity defined as injection rate rate divided by the bottom hole-reservoir pressure difference is small. It is therefore necessary in order to achieve a realistic field injection rate without exceeding the max. permissible bottom hole pressure to make sure that the total completed interval is sufficiently large. This may be accomplished by drilling more wells and/or reducing the well skin by acidizing etc.
- **Pore volume compressibility**
The pore volume compressibility has a large effect on injectivity as well as storage capacity. At the same time it is a parameter associated with a large uncertainty. There is a need to intensify the investigation of chalk behavior during decompression and compression.
- **Relative permeability**
The small relative permeabilities reduce the time span during which maximum injection rates can be maintained and thus the storage capacity
- **Bottom hole pressure limit**
Also the imposed upper limit of the bottom hole pressure has a direct influence on the time span during which the requested injection rate can be maintained. The higher the limit the longer the time span and the higher the storage capacity.

- Aquifer strength and extension
A correct description of the aquifer is important for the prediction of injectivity as well as storage capacity.

The capillary pressure was found to have little influence on the CO₂ injection conditions in the Roar field.

Factors which have not been investigated so far are:

- Geostatistical reservoir model
- Upscaled simulation grid
- Importance of free oil
- Solubility of CO₂ in water

It is expected that these conclusions hold in general for high-porosity/high-permeability unfractured chalk fields and thus also for the much larger Thyra field.

The estimated CO₂ storage capacity of the Roar field is 76 million tons at an abandonment pressure of 3000 psi (21 MPa).

References

Bech, N. & Frykman, P. 2002: Storage of CO₂ in depleted hydrocarbon reservoirs in low-permeability chalk. Sixth International Conference on Greenhouse Gas Control Technologies Kyoto, Japan RITE, IEA Greenhouse Gas R&D Program, JSER.1-4 oktober, 2002, 6 pp.

Calsep A/S 2001: PVTsim 11

Energistyrelsen 2002: Oil and Gas Production in Denmark

Foged, N. 2001: Personal communication, 29 November

Frykman, P. 2002: Upscaling of the Roar reservoir model, Danmarks og Grønlands Geologiske Undersøgelse Rapport 62, 13 pp.

If, F. 2002: CMoS: Chalk Model Synthesis tool for fracture analysis, flow upscaling and model conversion to finite difference flow simulation, COWI Consulting Engineers A/S, Lyngby.

Jakobsson, N.M. & Christian, T.M. 1994: Historical Performance of Gas Injection of Ekofisk, 69th SPE Annual Technical Conference and Exhibition, Houston, TX, 1994, (SPE Paper 28933).

Jensen, T.B., Harpole, K.J. & Østhus, A. 2000: EOR screening for Ekofisk, Proceedings of the European Petroleum Conference, Paris, France, 24-25 October 2000, 151-161 (SPE 65124).

Ruddy, I., Andersen, M.A., Patillo, P.D., Bishlawi, M. and Foged, N. 1989: Rock Compressibility, Compaction, and Subsidence in a High-Porosity Chalk reservoir: A case Study of Valhall Field, SPE 18278, Society of Petroleum Engineers 1989.

Schlumberger GeoQuest 2000: Eclipse Reservoir Simulators 2000A,

Todd, M. R. and Longstaff, W.J. 1972: The Development, Testing and Application of a Numerical Simulator for Predicting Miscible Flood Performance, SPE 3484, Feb. 1972

Vejbæk, O.V. 1999a: Reservoir characterization of the Roar field, Danmarks og Grønlands Geologiske Undersøgelse Rapport 59, 64 pp

Vejbæk, O.V. 1999b: Amendment to reservoir characterization of the Roar field, Danmarks og Grønlands Geologiske Undersøgelse Rapport 60, 13 pp.

Weir, G.J., White, S.P. and Kissling, W.M. 1996: Reservoir Storage and Containment of greenhouse Gases, *Transport in Porous Media* **23**, 37-60

List of Tables

Table 1. Produced volumes after five years (1 January 2001)

Table 2. Produced volumes and pressure after 16 years (1 January 2012)

List of Figures

Fig. 1. Roar 25 layer model, yz – cross section $i = 15$

Fig. 2. Saturation scaled relative permeabilities

Fig. 3. Gas and CO₂ formation volume factors

Fig. 4. Gas and CO₂ viscosities

Fig. 5. CO₂ injection rates

Fig. 6. Total volumes of CO₂ injected

Fig. 7. Influence of pore volume compressibility on production

Fig. 8. Influence of pore volume compressibility on injection

Fig. 9. Influence of pore volume compressibility on injection

Fig. 10. Two different CO₂/gas relative permeabilities.

Fig. 11. Influence of CO₂/gas relative permeability on injection

Fig. 12. Influence of gas – water capillary pressure on injection

Fig. 13. Influence of skin on injection

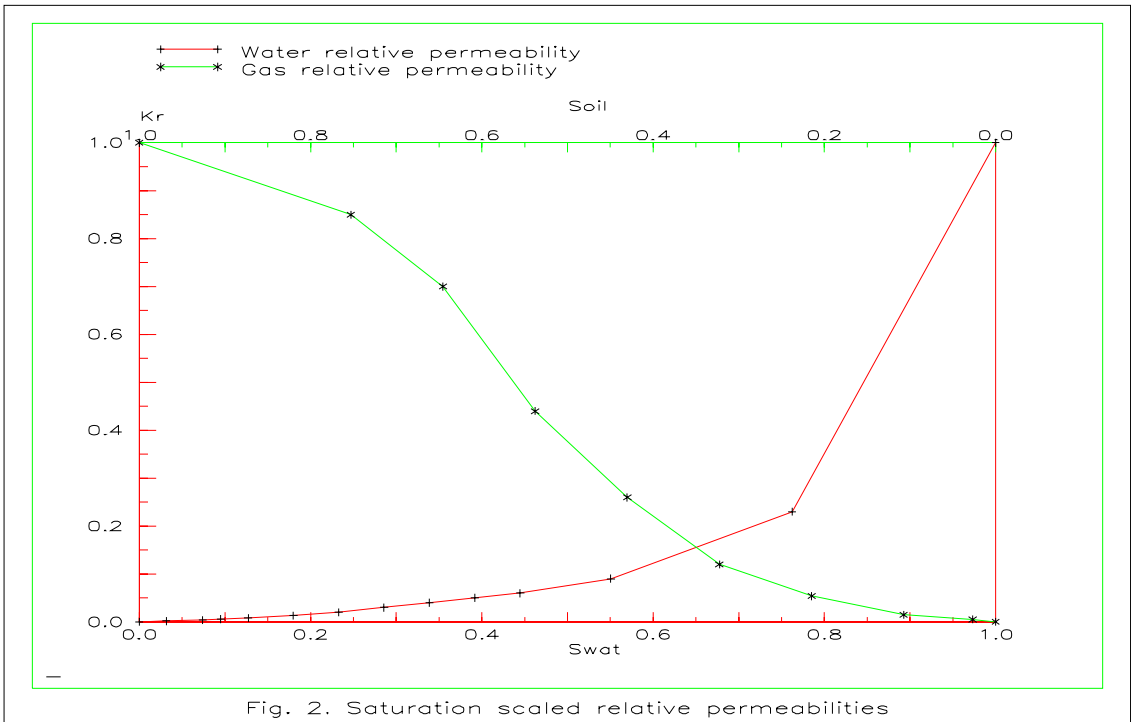
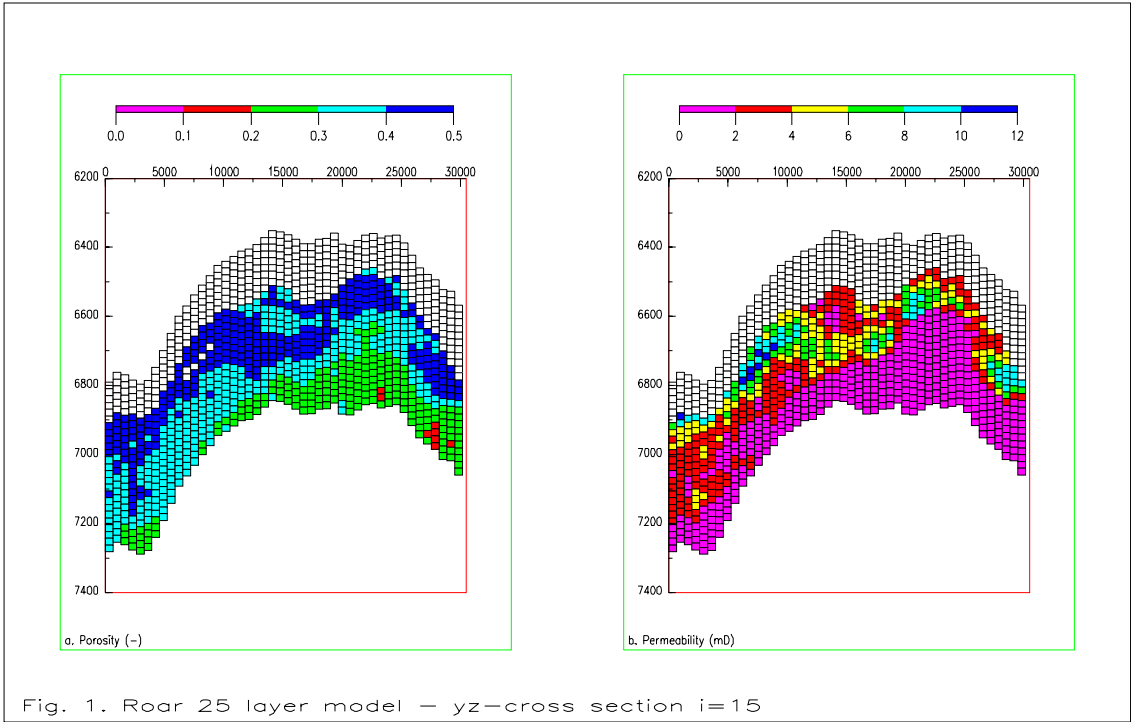
Fig. 14. Influence of aquifer permeability and extension

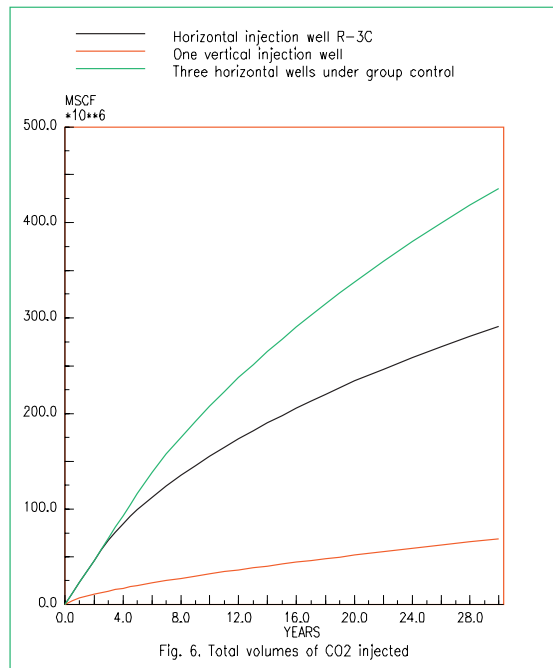
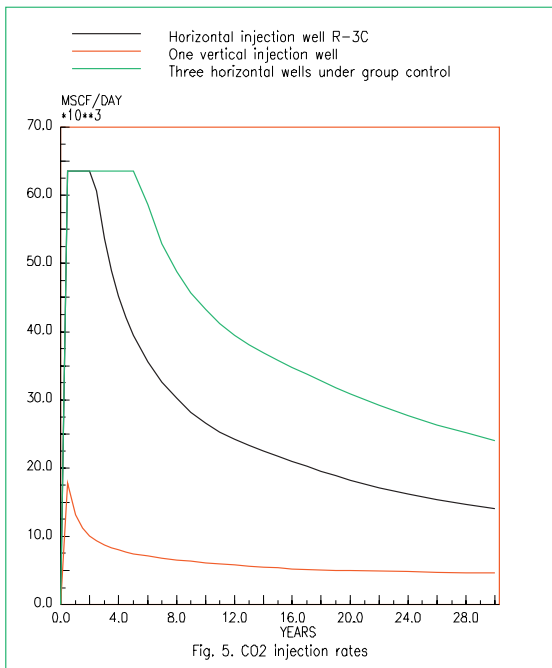
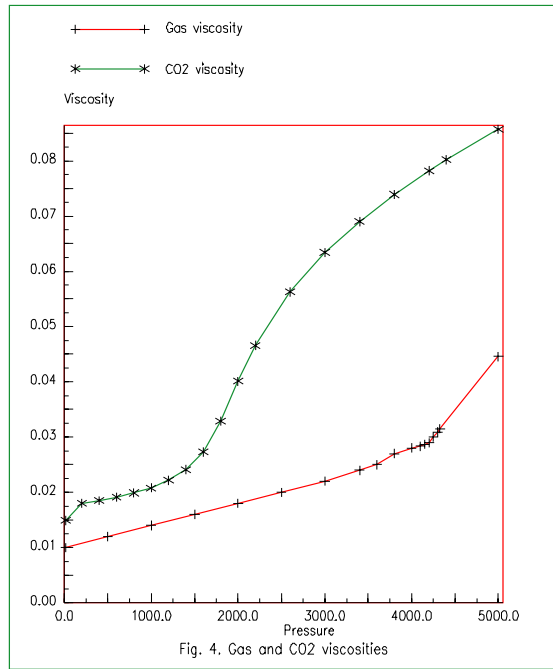
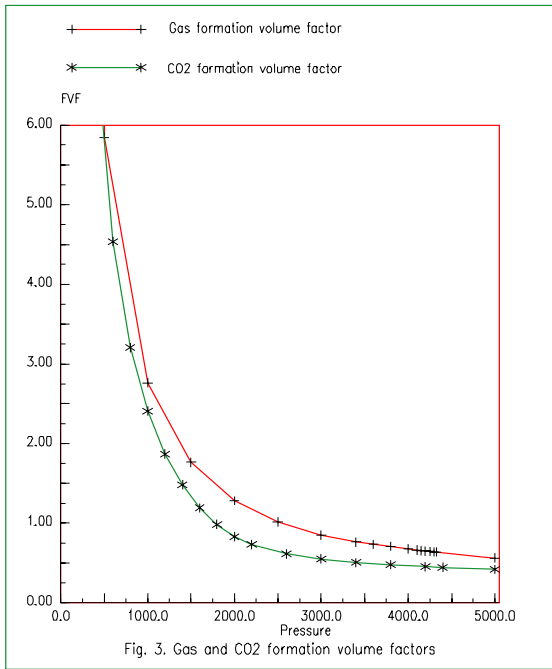
| | Unit | Recorded | Calculated with Crock = 5x10-5 | Calculated with Crock = 5x10-6 |
|-------|-----------------|----------------------|-----------------------------------|-----------------------------------|
| Oil | stb | 10.2x10 ⁶ | 8.52x10 ⁶ | 7.58x10 ⁶ |
| | sm ³ | 1.62x10 ⁶ | 1.35x10 ⁶ | 1.20x10 ⁶ |
| Gas | scf | 261.x10 ⁹ | 272.x10 ⁹ | 274.x10 ⁹ |
| | sm ³ | 7.40x10 ⁹ | 7.71x10 ⁹ | 7.77x10 ⁹ |
| Water | stb | 4.84x10 ⁶ | 7.64x10 ⁶ | 5.68x10 ⁶ |
| | sm ³ | 0.77x10 ⁶ | 1.21x10 ⁶ | 0.90x10 ⁶ |

Table 1. Produced volumes after five years (1 January 2001)

| | Unit | Calculated with Crock = 5x10-5 | Calculated with Crock = 5x10-6 |
|---------------------|-----------------|-----------------------------------|-----------------------------------|
| Oil | stb | 15.x10 ⁶ | 12.x10 ⁶ |
| | sm ³ | 2.3x10 ⁶ | 1.9x10 ⁶ |
| Gas | scf | 530x10 ⁹ | 543x10 ⁹ |
| | sm ³ | 15.x10 ⁹ | 15.10 ⁹ |
| Water | stb | 75.x10 ⁶ | 37.x10 ⁶ |
| | sm ³ | 12.x10 ⁶ | 5.9x10 ⁶ |
| Reservoir volume | rb | 456x10 ⁶ | 463x10 ⁶ |
| | m ³ | 72.x10 ⁶ | 74.x10 ⁶ |
| Pressure | psi | 3566 | 2787 |
| | MPa | 24.6 | 19.2 |

Table 2. Produced volumes and pressure after 16 years (1 January 2012)





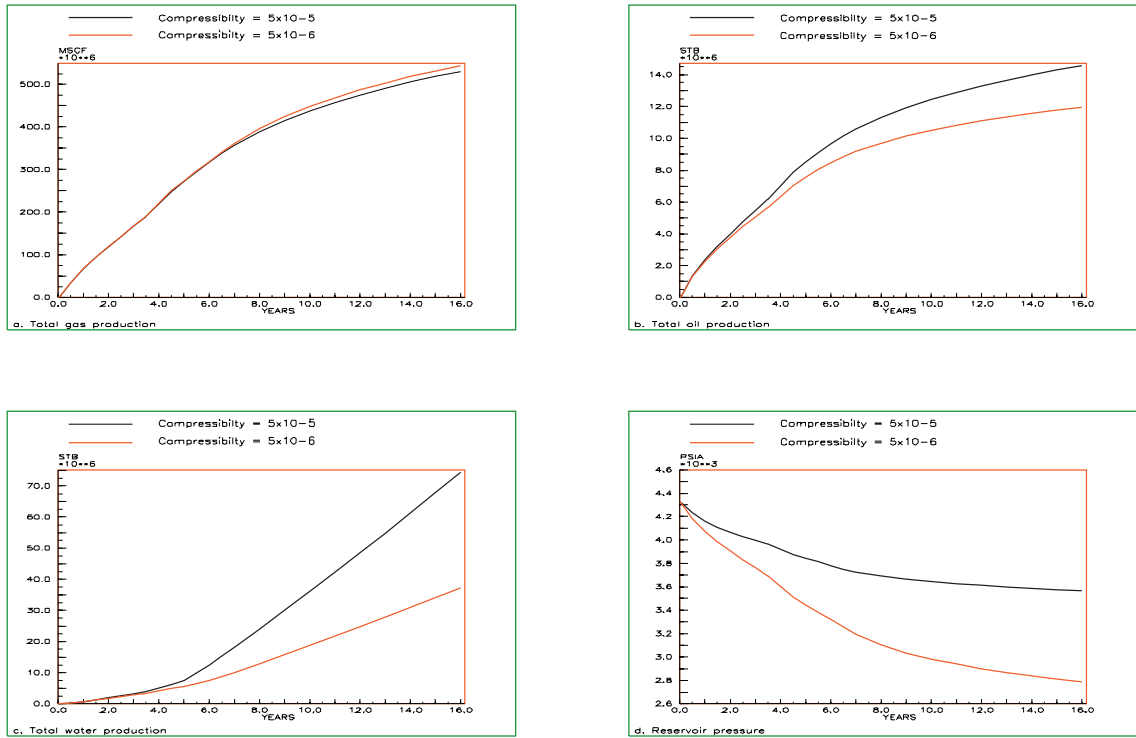


Fig. 7. Influence of pore volume compressibility on production

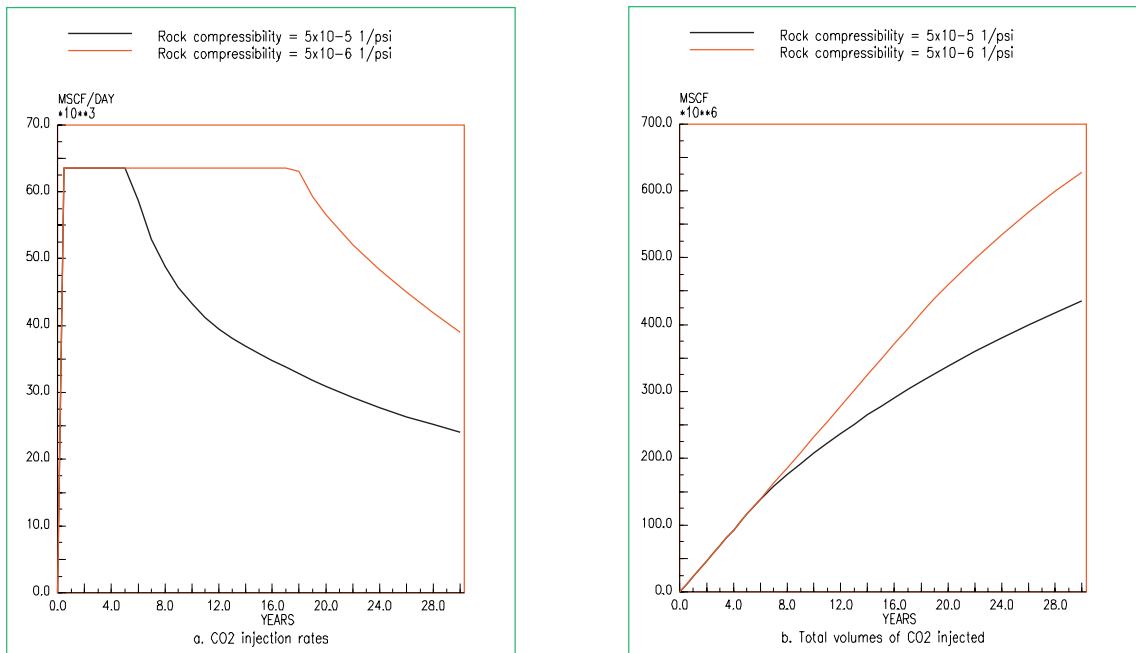


Fig. 8. Influence of pore volume compressibility on injection

Initial state based upon $C_{rock} = 5 \times 10^{-5} \text{ 1/psi}$

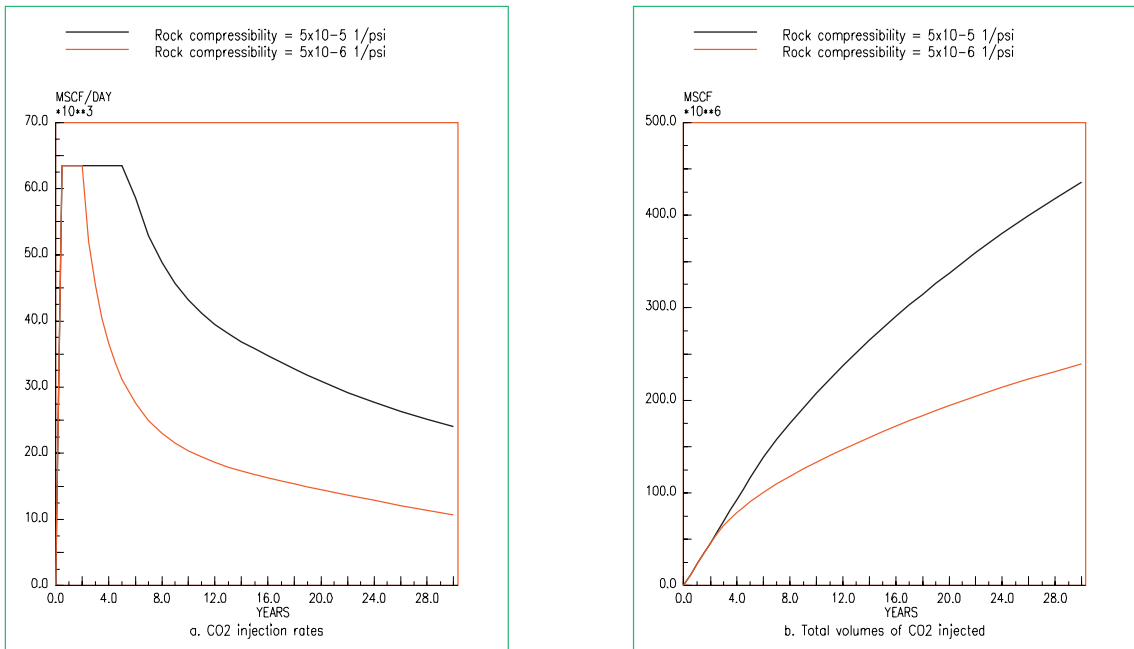


Fig. 9. Influence of pore volume compressibility on injection

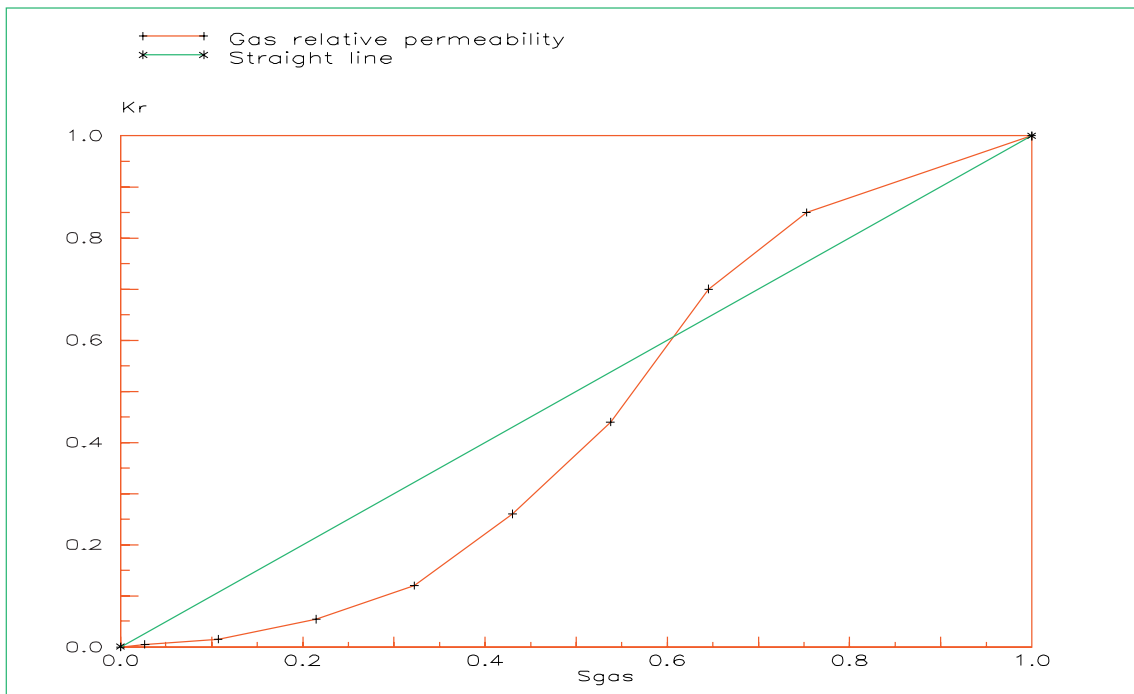


Fig. 10. Two different CO2 relative permeabilities.

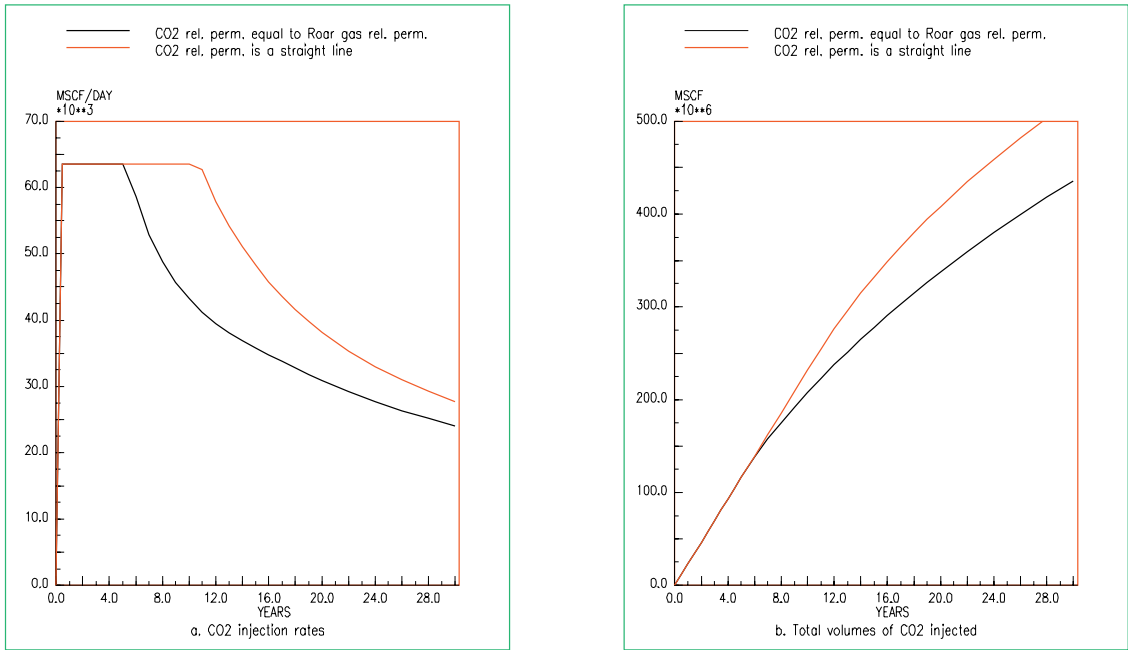


Fig. 11. Influence of CO2 relative permeability on injection

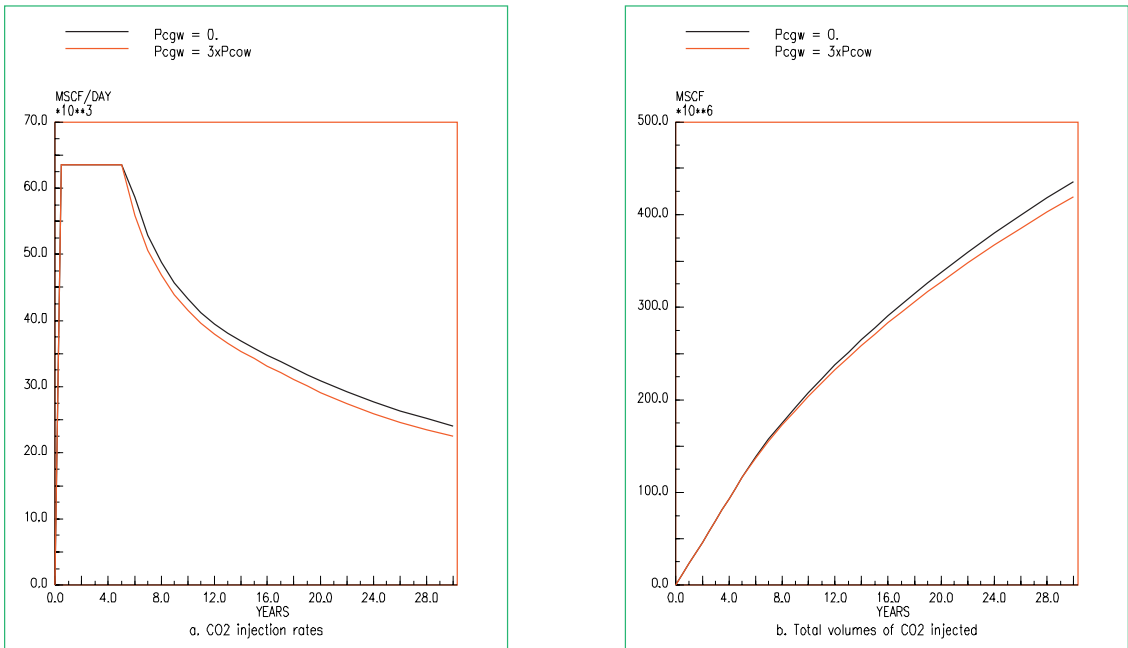


Fig. 12. Influence of gas-water capillary pressure on injection

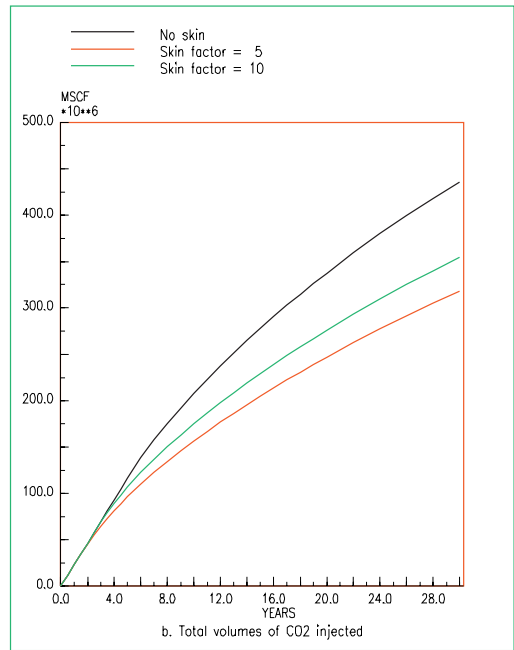
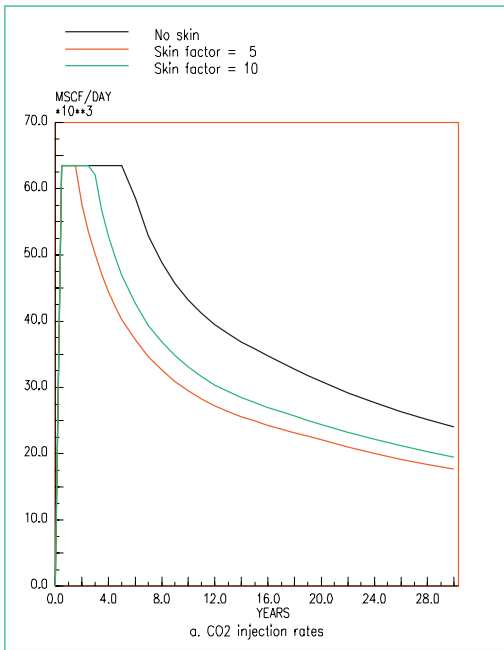


Fig. 13. Influence of skin on injection

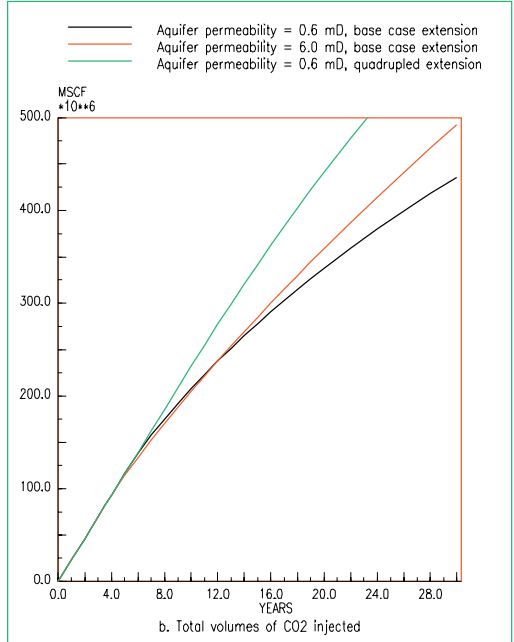
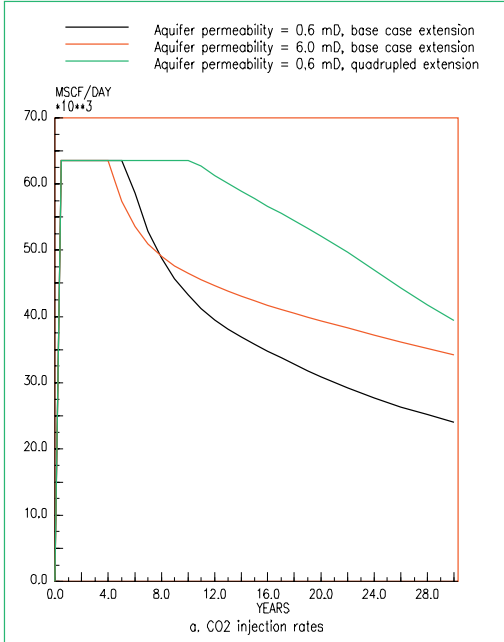


Fig. 14. Influence of aquifer permeability and extension